Rational Designs of Multifunctional Polymers

Wai-Kin Chan, Yongming Chen, Zhonghua Peng, and Luping Yu*

Contribution from the Department of Chemistry, The University of Chicago, 5735 South Ellis Avenue, Chicago, Illinois 60637

Received June 25, 1993®

Abstract: To manifest photorefractive effects, a polymer must possess a photocharge generator, a charge transporter, a charge trapping center, and a nonlinear optical chromophore. We utilized the Stille coupling reaction to synthesize a novel type of multifunctional polymer that contains a conjugated backbone and a second-order NLO chromophore. The expectation that the polymers will possess photorefractivity is the design idea behind the structure of the polymers. Because the conjugated backbone absorbs photons in the visible region and is photoconductive, it is expected to play the triple role of charge generator, charge transporter, and backbone. Thus, the four functionalities necessary to manifest the PR effect will exist simultaneously in a single polymer. The second harmonic generation and the photoconductivity measurements revealed that the polymers are nonlinear-optically active and photoconductive. Two beam-coupling experiments clearly indicated asymmetric optical energy exchange, which is an unambiguous demonstration of photorefractivity.

Introduction

In the past few decades, different polymeric materials have been synthesized and have demonstrated a variety of physical properties, such as liquid crystallinity,[1] electric conductivity,[2] photoconductivity,[3] semiconductivity,[3] nonlinear optical activity,[4,5] and piezoelectricity and pyroelectricity,[3] to name a few. Many of these properties are the basis for the modern advanced technology. However, the preparation of polymers that combine several of these properties together is a synthetic challenge requiring sophisticated molecular and/or supramolecular designs. Photorefractive polymers are multifunctional polymers that also possess photoconductivity and electrooptical activity.[6-8] To manifest photorefractive effects, the polymer must possess a photocharge generator, a charge transporter, a charge trapping center, and a nonlinear optical chromophore. Before 1990, photorefractive studies had mainly focused on inorganic materials. In the past 3 years, polymeric composite materials have been studied for photorefractivity.[9] While these composite systems enjoy the ease of preparation, problems, such as phase separations and the instability of electrooptical activities, make it desirable to synthesize photorefractive polymers in which all of the species are covalently attached.

We have succeeded in synthesizing such novel photorefractive polymers which contain an NLO chromophore, a charge generator, and a transporting compound covalently linked to the polymer backbone.[10,11] Two beam coupling experiments revealed that the refractive index grating, caused by the space charge field with a phase shift of 90°, is a major contribution to the optical gain. This demonstrated the photorefractive effect.

There are two common features of our previous photorefractive polymers' structures.[11,12] First, a comonomer (diisocyanate in this case) was used to link the different species; therefore, the density of the different species is limited to a low level. To optimize the PR effect, the densities of the charge generator, the charge transporter, and the NLO chromophore should be optimized. Second, the polymer backbones were polyurethanes that cannot effectively transport photocharge carriers. The charge carriers in these materials were transported by a hopping mechanism. It is known that in order to achieve an effective space charge field, the charge must be separated by at least half a wavelength. This clearly requires charge carriers to experience many cycles of hop/trap/reexcitation, resulting in a small mobility and slow buildup time for the space charge field. This property might be desired for information storage because the charge separation can remain for a long time. However, it is not appropriate for fast information processing that requires a fast response time.

A novel type of PR polymer, containing a conjugated backbone, a second-order NLO chromophore and a small amount of charge trapper (see Scheme I), may solve these problems. The conjugated backbone absorbs photons in the visible region and can play the triple role of charge generator, charge transporter, and backbone. It is known that conjugated polymers have relatively high photogenerated carrier mobility (10^{-3}–10^{-5} $cm^2/(V\cdot s)$).[2,3] Thus, the four functionalities necessary to manifest the PR effect will exist simultaneously in a single polymer. Recent experiments have shown that the polythiophene oligomer has a mobility close to 0.1 $cm^2/(V\cdot s)$.[12] Therefore, conjugated PR polymers could have a much larger mobility and a faster response time than any other PR polymer ever reported.

In order to synthesize these materials, new chemistry is required because the usual polymerization chemistry, such as Zigler–Natta polymerization,[13] electrochemical polymerization, and oxidative

* Abstract published in *Advance ACS Abstracts*, November 15, 1993.

(1) Weiss, R. A.; Ober, C. K., Eds., *Liquid Crystal Polymers*; ACS Symp. Series No. 435; American Chemical Society: Washington, DC, 1990.

(2) Skotheim, T. A. *Handbook of Conductive Polymers*; Marcel Dekker: New York and Basel; 1986; Vols. 1 and 2.

(3) Mort, J.; Pfister, G., Eds. *Electronic Properties of Polymers*; John Wiley and Sons: New York, 1982.

(4) Marder, S. R.; Sohn, J. R.; Stucky, G. D. *Materials for Nonlinear Optics*; ACS Symp. Series No. 455; American Chemical Society: Washington, DC, 1991.

(5) Chemla, D. S.; Zyss, J., Eds. *Nonlinear Optical Properties of Organic Molecules and Crystals*; Academic Press: New York, 1987; Vols 1 and 2.

(6) Gunter, P.; Huiguard, J. P. Eds. *Photorefractive Materials and Their Applications*; Springer-Verlag: Berlin, 1988; Vols. I and II.

(7) Yariv, A. *Optical Electronics*, 4th ed.; Saunders College Publishing: Philadelphia, 1991.

(8) Sutter, K.; Hullinger, J.; Gunter, P. *Solid State Commun.* **1986**, *74*, 867.

(9) (a) Ducharme, S.; Scott, J. C.; Twieg, R. J.; Moerner, W. E. *Phys. Rev. Lett.* **1991**, *66*, 1846. (b) Walsh, C. A.; Moerner, W. E. *J. Opt. Soc. Am. B* **1992**, *9*, 1642. (c) Silence S. M.; Walsh, C. A.; Scott, J. C.; Moerner, W. E. *Appl. Phys. Lett.* **1992**, *61*, 2967. (d) Cui, Y. P.; Zhang, Y.; Prasad, P. N. *Appl. Phys. Lett.* **1992**, *61*, 2132. (e) Tamura, K.; Padias, A. B.; Hall, H. K., Jr.; Peyghambarian, N. *Appl. Phys. Lett.* **1992**, *60*, 1803.

(10) Yu, L. P.; Chan, W. K.; Bao, Z. N.; Cao, S. *J. Chem. Soc., Chem. Commun* **1992**, 1735.

(11) Yu, L. P.; Chan, W. K.; Bao, Z. N.; Cao, S. *Macromolecules* **1993**, *26*, 2216.

(12) Peng, X.; Horowitz, G.; Fichou, D.; Garnier, F. *Appl. Phys. Lett.* **1990**, *57*, 2013.

(13) Ordian, G. *Principles of Polymerization*, 2nd ed.; John Wiley & Sons: New York 1981.

0002-7863/93/1515-11735$04.00/0 © 1993 American Chemical Society

Scheme I. Schematic Structure of Conjugated Photorefractive Polymer

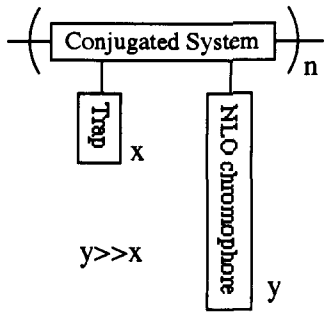

coupling reaction,[2,14] cannot tolerate the many functional groups necessary for the introduction of different moieties. However, in the course of searching for novel nonlinear optical polymers, we found that the Stille reaction offers the solution to this problem.[15] These palladium-catalyzed reactions between organic halides (or triflate) and organotin compounds are very versatile in synthesizing functional polymers (see Scheme II). The reaction conditions are very mild, and the reaction yield is usually high.[16,17] Best of all, this reaction can tolerate different substituents of the monomers, such as amines, alcohols, esters, ethers, etc., allowing us to introduce different functionality into the polymer backbone. We utilized this reaction to synthesize multifunctional polymers that two-beam coupling experiments have demonstrated to be photorefractive. This paper reports the detailed synthesis and characterizations of these multifunctional polymers.

Experimental Section

Dioxane was purified by distillation over calcium hydride and stored with a 3-Å molecular sieve. All of the other chemicals were purchased from the Aldrich Chemical Co. and were used as received unless otherwise stated. The synthetic schemes for monomer synthesis are shown as Schemes III and IV.

Synthesis of Monomers: Compound 1. *n*-Butyl lithium (2.5 M, 68 mL, 171 mmol) was added to a solution of 1,4-dimethoxybenzene (23.6 g, 171 mmol) in THF (40 mL) in a 500-mL two-necked round-bottom flask at 0 °C. The solution was stirred for 1 h and then transferred dropwise into a solution of 1,6-dibromohexane (33.2 mL, 205 mmol) in THF (20 mL) in another round-bottom flask. The resulting mixture was stirred at room temperature for 1 h and then poured into water (100 mL). The mixture was extracted with diethyl ether (3 × 30 mL); the organic layers were combined, washed with a saturated sodium chloride solution (30 mL), and dried over magnesium sulfate. After removal of the solvent, the crude product was vacuum distilled to yield a colorless liquid, compound **1** (28.5 g, 55%): bp 155–160 °C (1 Torr). ^{1}H NMR ($CDCl_3$, ppm): δ 1.34–1.86 (m, -C_4H_8-, 8 H), 2.56 (t, J = 7.6 Hz, Ar-CH_2-, 2 H), 3.38 (t, J = 6.8 Hz, Br-CH_2-, 2 H), 3.74 (s, CH_3O-, 3 H), 3.75 (s, CH_3O-, 3 H), 6.63–6.73 (m, ArH, 3 H).

Compound 2. In a 100-mL round-bottom flask, a solution of compound **1** (10.00 g, 33.2 mmol), *N*-methylaniline (5.40 mL, 49.8 mmol), potassium carbonate (9.20 g, 66.4 mmol), tetrabutylammonium bromide (0.54 g, 1.7 mmol), and sodium iodide (10 mg, 0.07 mmol) in toluene (10 mL) was stirred under reflux for 5 h. Diethyl ether (25 mL) and water (25 mL) were added. The organic layer was separated and dried over magnesium sulfate. After removal of the solvent, the unreacted starting material was distilled out under a vacuum (50 °C (1 Torr)); compound **2** was collected as residue (10.00 g, 92%). ^{1}H NMR ($CDCl_3$, ppm): δ 1.34–1.58 (m, -C_4H_8-, 8 H), 2.55 (t, J = 6.3 Hz, Ar-CH_2-, 2 H), 2.87 (s, N-CH_3, 3 H), 3.25 (t, J = 6.7 Hz, -NCH_2-, 2 H), 3.71 (s, CH_3O-, 3 H), 3.72 (s, CH_3O-, 3 H), 6.61–6.70 (m, ArH, 6 H), 7.14–7.17 (m, ArH, 2 H).

Compound 3. Phosphorus oxychloride (1.4 mL, 15.3 mmol) was added dropwise to DMF (4.7 mL, 61.2 mol) at 0 °C. The solution was stirred at 0 °C for 1 h and then at 25 °C for 1 h more. Compound **2** (5.00 g, 15.3 mmol) was then added dropwise to the mixture. The resulting solution was stirred at 90 °C for 4 h. After being cooled down to room temperature, the solution was poured into an ice–water mixture which was then neutralized with a saturated sodium acetate solution and extracted with dichloromethane (3 × 20 mL). The combined organic solution was washed with water (2 × 25 mL) and then with a saturated sodium chloride solution (25 mL). After removal of the solvent, the crude product was chromatographed using a silica gel column, using hexane/ethyl acetate (2:1) as the eluent, affording a pale yellow liquid compound **3** (2.40 g, 45%). ^{1}H NMR ($CDCl_3$ ppm): δ 1.34–1.58 (m, -C_4H_8-, 8 H), 2.56 (t, J = 6.3 Hz, Ar-CH_2-, 2 H), 3.01 (s, NCH_3, 3 H), 3.37 (t, J = 7.5 Hz, NCH_2-, 2 H), 3.73 (s, -OCH_3, 3 H), 3.74 (s, -OCH_3, 3 H), 6.62–6.70 (m, ArH, 5 H), 7.66 (d, J = 8.6 Hz, ArH, 2 H), 9.66 (s, -CHO, 1 H).

Compound 4. Sodium hydride (0.36 g, 15 mmol) was added to a solution of compound **3** (2.7 g, 7.5 mmol) in 1,2-dimethoxyethane (5 mL). The solution was stirred for 5 min and diethyl 4-(methylsulfonyl)-benzyl phosphate (2.3 g, 7.5 mmol) was added dropwise. The red solution was stirred at 75 °C for 10 h. The solution was poured into crushed ice (50 g) under nitrogen and then extracted with dichloromethane (3 × 20 mL). The combined organic solution was washed with water (30 mL) and brine (30 mL). After removal of the solvent, the crude product was chromatographed in a silica gel column, using CH_2Cl_2/MeOH (100:1) as the eluent, to give a bright yellow liquid (4) (1.6 g, 63%). ^{1}H NMR ($CDCl_3$, ppm): δ 1.34–1.58 (m, -C_4H_8-, 8 H), 2.56 (t, J = 7.5 Hz, Ar-CH_2-, 2 H), 2.96 (s, -NCH_3, 3 H), 3.04 (s, -SO_2CH_3, 3 H), 3.32 (t, J = 7.5 Hz, -NCH_2-, 2 H), 3.73 (s, -OCH_3, 3 H), 3.74 (s, -OCH_3, 3 H), 6.62–6.73 (m, ArH, 5 H), 6.85 (d, J = 16.2 Hz, -HC═, 1 H), 7.13 (d, J = 16.2 Hz, -HC═, 1 H), 7.36–7.81 (m, ArH, 6 H).

Compound 5. Compound **4** (1.6 g, 3.2 mmol) in dichloromethane (10 mL) was added slowly to a BBr_3/CH_2Cl_2 solution (1.7M, 5.7 mL, 9.6 mmol) at −78 °C. After the addition was complete, the solution was warmed up slowly to room temperature and stirred for 24 h. The solution was then added to an ice–water mixture with vigorous stirring and the organic layer was separated, washed with water (25 mL), and dried over magnesium sulfate. After removal of the solvent, the crude product was separated in a silica gel column, using hexane/ethyl acetate (1:2) as the eluent, to give a viscous yellow liquid (1.2 g, 80%). ^{1}H NMR ($CDCl_3$, ppm): δ 1.34–1.58 (m, -C_4H_8-, 8 H), 2.52 (t, J = 7.5 Hz, Ar-CH_2-, 2 H), 2.92 (s, -NCH_3, 3 H), 3.02 (s, -SO_2CH_3, 3 H), 3.28 (t, J = 7.5 Hz, -NCH_2-, 2 H), 5.39 (br s, -OH, 1 H), 5.71 (br s, -OH, 1 H), 6.56–6.61 (m, ArH, 5 H), 6.82 (d, J = 16.2 Hz, -HC═, 1 H), 7.10 (d, J = 16.2 Hz, -HC═, 1 H), 7.34 (d, J = 8.4 Hz, ArH, 2 H), 7.51 (d, J = 8.1 Hz, ArH, 2 H), 7.78 (d, J = 8.1 Hz, ArH, 2 H).

Monomer A. Trifluoromethanesulfonic anhydride (1.9 ml, 11.7 mmol) was added slowly to a solution of compound **5** (1.90 g, 3.9 mmol) in pyridine (15 mL) at −20 °C. The solution was stirred at room temperature for 24 h and then poured into water (20 mL) and extracted with dichloromethane (3 × 20 mL). The combined organic layer was washed with water (3 × 20 mL) and dried over magnesium sulfate. After removal of the solvent, the crude product was separated in a solica gel column, using hexane/ethyl acetate (2:1) as the eluent. The product collected was recrystallized again with methanol to yield 1.30 g of a yellow solid (45%): mp, 94–96 °C. ^{1}H NMR ($CDCl_3$, ppm): δ 1.34–1.58 (m, -C_4H_8-, 8 H), 2.72 (t, J = 7.8 Hz, Ar-CH_2-, 2 H), 2.96 (s, -NCH_3, 3 H), 3.04 (s, -SO_2CH_3, 3 H), 3.34 (t, J = 7.3 Hz, -NCH_2-, 2 H), 6.63 (d, J = 8.0 Hz, ArH, 2 H), 6.85 (d, J = 16.2 Hz, -HC═, 1 H), 7.13 (d, J = 16.2 Hz, -HC═, 1H), 7.16–7.31–7.81 (m, ArH, 9 H). Calcd for $C_{30}H_{31}NF_6O_8S_3$: C, 48.45; H, 4.20; N, 1.88. Found: C, 47.96; H, 4.08; N, 1.99.

Compound 8. Compound **7**[18] (0.73 g, 2.1 mmol) and sodium hydride (0.13 g, 5.3 mmol) were added to DMF (8 mL). The solution was heated to reflux for 2 h. It was then cooled down to room temperature and 1-bromohexane (0.88 g, 5.3 mmol) was added. The resulting mixture was heated under reflux for an additional 3 h. After being cooled down to room temperature, the solution was filtered and the solid filtered was washed with chloroform. The filtrate was then washed with water (3 × 20 mL). The organic solution was dried over anhydrous sodium sulfate. After removal of the solvent, the solid collected was recrystallized with methanol to afford compound **8** (0.20 g, 20%). ^{1}H NMR ($CDCl_3$, ppm): δ 0.80 (t, J = 6 Hz, CH_3-, 6 H), 1.20–1.65 (m, -$(CH_2)_4$-, 16 H), 3.75 (t, J = 7 Hz, -NCH_2-, 4 H), 3.90 (s, -OCH_3, 6 H), 7.00 (d, J = 9 Hz, ArH, 4 H), 7.8 (d, J = 9 Hz, ArH, 4 H).

Compound 9. Boron tribromide (7.2 mL, 12 mmol) in CH_2Cl_2 (10 mL) was added slowly to a solution of compound **8** (1.00 g, 2.0 mmol)

(14) Roncali, J. *Chem. Rev.* **1992**, *92*, 711.
(15) Bao, Z. N.; Chan, W. K.; Yu, L. P. *Chem. Mater.* **1993**, *6*, 2.
(16) Stille, J. K. *Angew. Chem., Int. Ed. Engl.* **1986**, *25*, 508.
(17) Echavarren, A. M.; Stille, J. K. *J. Am. Chem. Soc.* **1987**, *109*, 5478.
(18) Potrawa, T.; Langhals, H. *Chem. Ber.* **1987**, *120*, 1075.
(19) Bao, Z. N.; Yu, L. P., manuscript in preparation.

Scheme II. Polymerization Utilizing the Stille Coupling Reaction

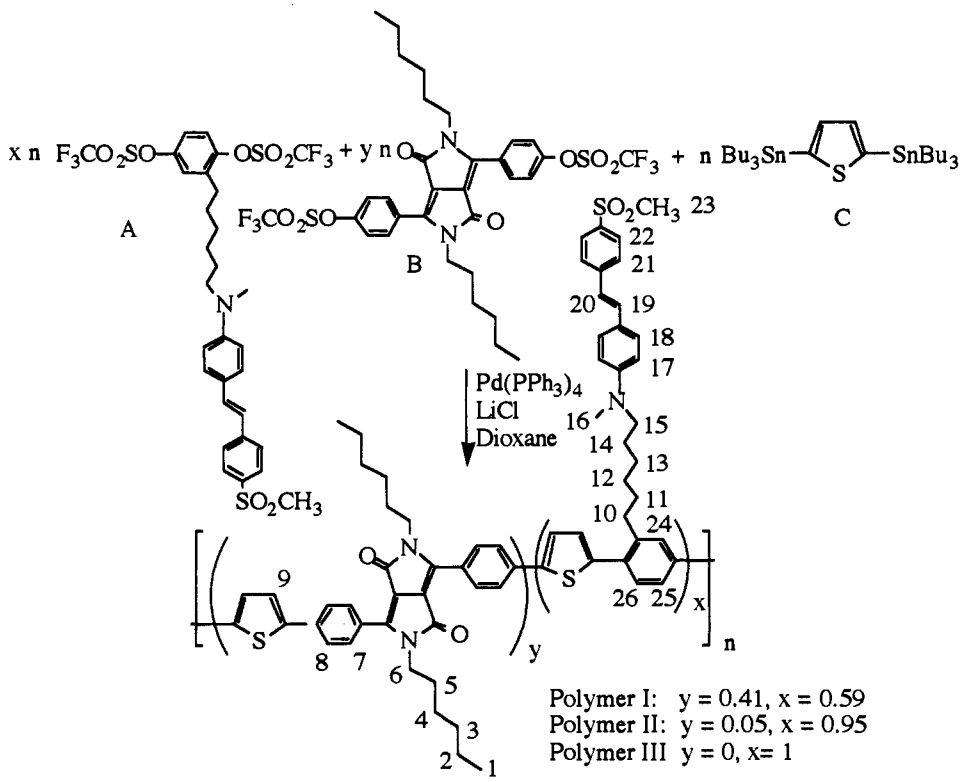

Scheme III. Synthesis of Monomer A

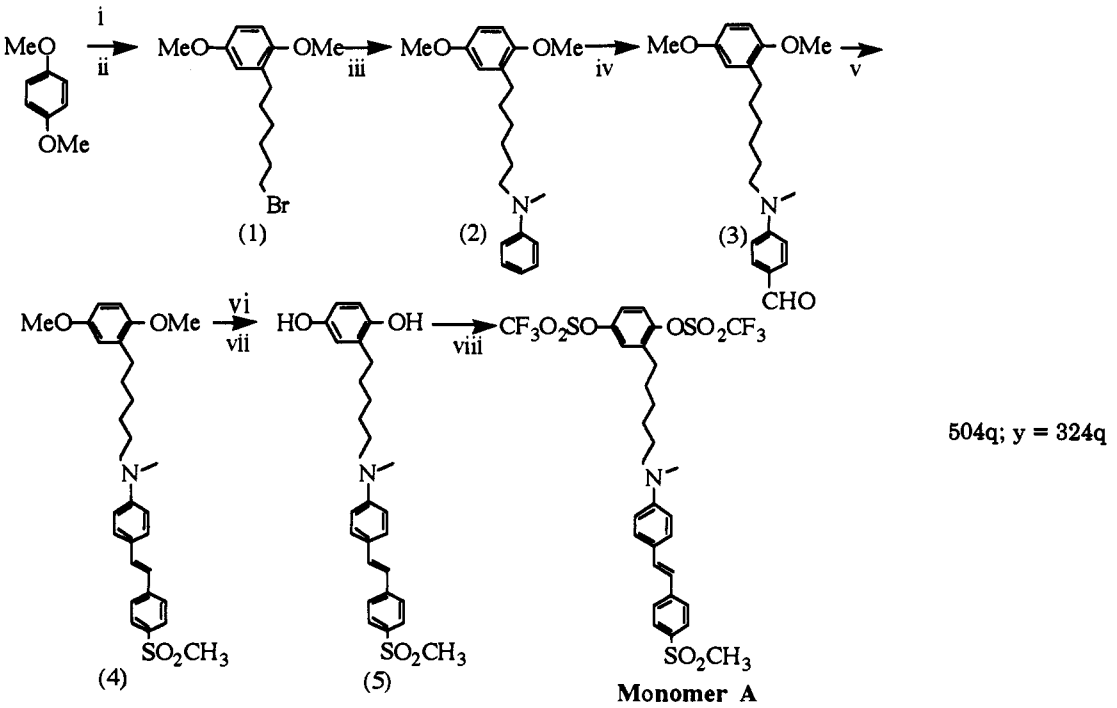

Reaction conditions:
i. LiBu/THF, ii, 1,6-dibromohexane, iii, N-methylaniline/NBu_4Br/Na_2CO_3/Toluene,
iv. POCl3/DMF, v, diethyl 4-(methylsulfonyl)bezyl phosphate/NaH/Glyme,
vi, BBr_3/CH_2Cl_2, vii, H_2O, viii, Pyridine/trifluromathanesulfonic anhydride.

in CH_2Cl_2 (10 mL) at −78 °C. The solution was gradually warmed up to room temperature and stirred for 24 h. Water (10 mL) was added slowly to the solution. The resulting mixture was extracted with dichloromethane (3 × 20 mL). The combined organic layer was dried over magnesium sulfate and concentrated. The crude product was recrystallized with DMSO, yielding compound **9** as a red solid (0.79 g, 82%). ^{1}H NMR (DMSO-d_6, ppm): δ 0.75 (t, J = 6.6 Hz, CH_3-, 6 H), 1.10–1.40 (m, -$(CH_2)_4$-, 16 H), 3.66 (t, J = 7 Hz, -NCH_2-, 4 H), 6.87 (d, J = 9 Hz, ArH, 4 H), 7.66 (d, J = 9 Hz, ArH, 4 H), 9.45 (br s, -OH, 2 H).

Monomer B. Trifluoromethanesulfonic anhydride (0.66 mL, 3.9 mmol) was added slowly to a solution of compound **9** (0.75 g, 1.56 mmol) in

504q; y = 324q

Scheme IV. Synthesis of Monomer B

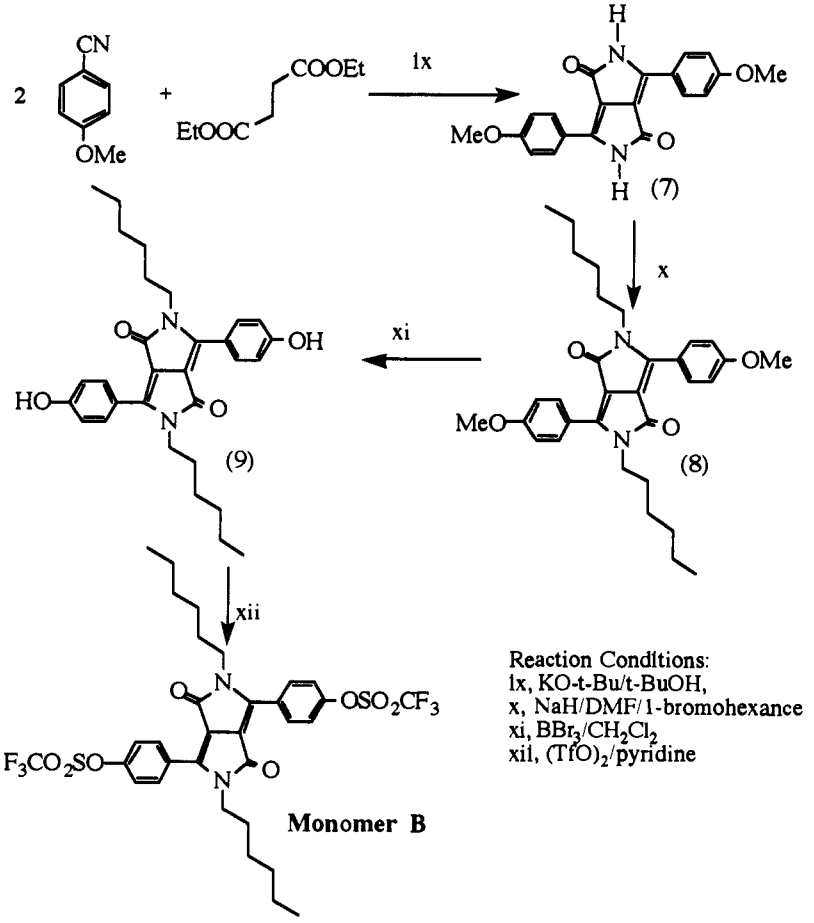

pyridine (5 mL) at 0 °C. The resulting solution was stirred at room temperature for 24 h. The color of the solution turned from red to light green during the course of the reaction. The solution was poured into water (10 mL), and the solid was filtered, washed with water, and then recrystallized with a mixture of methanol and chloroform. Compound **10** was collected as yellow needle-shaped crystals (1.1 g, 94%, mp 149–151 °C). ^{1}H NMR ($CDCl_3$, ppm): δ 0.80 (t, J = 6.6 Hz, -CH_3, 6 H), 1.25–1.55 (m, -$(CH_2)_4$-, 16 H), 3.70 (t, J = 7 Hz, -NCH_2-, 4 H), 7.40 (d, J = 9 Hz, ArH, 4 H), 7.90 (d, J = 9 Hz, ArH, 4 H). Calcd for $C_{32}H_{34}N_2F_6O_8S_2$: C, 51.06; H, 4.55; N, 3.72. Found: C, 50.76; H, 4.23; N, 3.76.

Polymerization. A typical polymerization procedure is exemplified by that for polymer I. To a 25-mL two-necked round-bottom flask were added monomer A (0.296 g, 0.398 mmol), monomer B (0.210 g, 0.279 mmol), 2,5-bis(tributylstannyl)thiophene[15] (monomer C, 0.448 g, 0.677 mmol), lithium chloride (86 mg, 2.0 mmol), tetrakis(triphenylphosphine)-palladium(0) (16 mg, 2 mol %), and 1,4-dioxane (4 mL). The mixture was heated at 90 °C for 16 h, and the polymer was precipitated into methanol and collected by filtration (almost quantitative yield). To further purify the polymer, it was dissolved in NMP and precipitated again into acetone. After being further washed with acetone in a Soxhlet extractor for 2 days, the polymer was collected as a dark red solid. The ^{1}H NMR data for polymers I–III are as follows (the numbering refers to Scheme II). Polymer I (CD_5Cl, ppm): δ 0.90 (b, H_1), 1.25 (b, H_2-H_4), 1.40–1.80 (b, H_5, H_{11}–H_{14}), 2.80 (s, H_{10}), 2.90 (s, H_{16}), 3.05 (s, H_{23}), 3.30 (s, H_{15}), 4.05 (b, H_6), 6.4 (b, H_{17}), 6.55 (d, J = 16.5 Hz, H_{19}), 6.75 (d, J = 16.5 Hz, H_{20}), 7.0–8.2 (b, heavily overlapped with solvent peaks, aromatic). Polymer II ($CDCl_3$, ppm): δ 0.89 (b, H_1), 1.30 (b, H_2–H_4), 1.40–1.70 (b, H_5, H_{11}–H_{14}), 2.75 (t, J = 7.8 Hz, H_{10}), 2.95 (s, H_{16}), 3.05 (s, H_{23}), 3.35 (t, J = 7.2 Hz, H_{15}), 6.65 (d, J = 8.1 Hz, H_{17}), 6.90 (d, J = 16.5 Hz, H_{19}), 7.15 (d, J = 16.5 Hz, H_{20}), 7.30 (m, H_9), 7.40 (d, J = 8.1 Hz, H_{18}), 7.52 (m, $H_{7,8}$), 7.55 (d, J = 8.3 Hz, H_{21}), 7.85 (d, J = 8.3 Hz, H_{22}). Polymer III ($CDCl_3$, ppm): δ 1.40, 1.65, 1.70 (b, H_{11}–H_{14}), 2.75 (t, J = 7.8 Hz, H_{10}), 2.95 (s, H_{16}), 3.05 (s, H_{23}), 3.35 (t, J = 7.2 Hz, H_{15}), 6.65 (d, J = 8.1 Hz, H_{17}), 6.90 (d, J = 16.5 Hz, H_{19}), 7.15 (d, J = 16.5 Hz, H_{20}), 7.30 (m, H_9), 7.40 (d, J = 8.1 Hz, H_{18}), 7.55 (d, J = 8.3 Hz, H_{21}), 7.85 (d, J = 8.3 Hz, H_{22}).

Characterization. The ^{1}H NMR spectra were collected on a Varian 400-MHz FT NMR spectrometer. The FTIR spectra were recorded on a Nicolet 20 SXB FTIR spectrometer. A Perkin-Elmer Lambda 6 UV/vis spectrophotometer was used to record the UV/vis spectra. Thermal analyses were performed by using the DSC-10 and TGA-50 systems from TA Instruments under a nitrogen atmosphere. The polarizing microscopic observation was performed with a Nikon (HFX-IIA) microscope equipped with a Linkam (TMS-90) hot stage. The intrinsic viscosity was obtained in a constant temperature bath (30 °C) using a Ubbelohde viscometer; NMP was used as the solvent. The GPC measurements were performed on a Waters RI system equipped with an UV detector, a differential refractometer detector, and an Ultrastyragel linear column at 35 °C using THF (HPLC grade; Aldrich) as an eluant. The molecular weight and the molecular weight distribution were calculated on the basis of monodispersed polystyrene standards.

The photoconductivity was studied by measuring the voltage resulting from a photocurrent run through the sample and across a 10-kΩ resistor.[14] A He–Ne laser (623.8 nm) with an intensity of 0.096 W/cm^2 was used as the light source. The carrier mobility was characterized by a conventional time-of-flight method.[12,13] The polymer films (about 1.4 μm) were cast on ITO covered glass slides. A semitransparent gold layer was thermally evaporated onto the polymer surface. A 337-nm nitrogen laser with a pulse width of 3 ns (Laser Science, Inc., Model 337) was directed onto the gold electrode; a sheet of charge carriers was generated near the electrode. The charge carriers drifted across the sample under the influence of an electrical field. When the resistor R was properly chosen so that RC constant was much less than the transit time τ, the voltage across R was proportional to the current passing through the sample. When the carriers exited the sample at the second electrode, the current rapidly dropped. The transit time related to the mobility by $\tau = L/\mu E$ was determined by a digitized oscilloscope (Tektronix Model TDS 540), where L is the thickness of the sample and E is the field strength.

Second-order NLO properties of poled polymeric films were characterized by second harmonic generation experiments. A mode-locked Nd:YAG laser (Continuum-PY61C-10, 10-Hz repetition rate) was used as the light source. The second harmonic generated by the fundamental

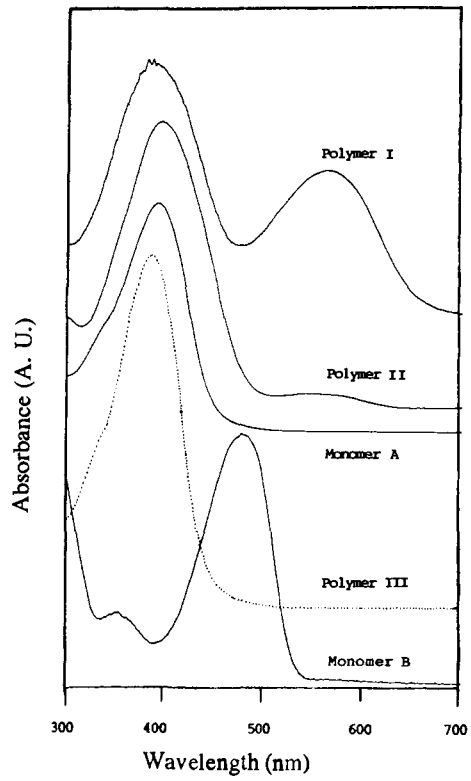

Figure 1. UV/vis spectra of monomers A and B, polymers I–III. The monomer spectra were taken in THF and the polymer spectra were taken in thin films.

wave (1064 μm) was detected by a photomultiplier tube (PMT) and then amplified and averaged in a boxcar integrator.

The linear electrooptic coefficient, r_{33}, of the poled films was measured at a wavelength of 0.633 μm using an reflection method developed by Teng et al.[20] A soleil-Babinet compensator was used to bias the DC intensity at half maximum intensity. The phase retardation between the p and s waves was modulated at about 7 kHz. The modulation of the intensity amplitude was determined using a lock-in amplifier, which can be used to calculate the r_{33} values.

A two-beam coupling experiment was performed using an electrically poled polymer sample (polymer I, thickness, 7 μm; r_{33}, 2.1 pm/V; poling temperature, 130 °C; poling voltage, ca 3.5 kV; poling time, 3 h). A diode laser (690 nm, 25 mW, Laser Power Technology, 690-300 was used as the laser source. The laser beam was equally split into two beams (each with intensity of 244 mW/cm^2, s-polarization), which were intersected on the polymer sample at 32°. To utilize the r_{33} value, the polymer film was tilted as shown in Figure 12. The transmitted intensities of the two beams were monitored using two diode detectors.

Results and Discussion

Designs of Monomers and Polymers. From our previous work,[15] we found that poly(2,4-dialkoxy-1,4-phenylene-*co*-2,5-thiophene) has an absorption maximum at 461 nm and a band-edge of 532 nm and it is photoconductive. Therefore, this conjugated backbone satisfies our requirements for being a charge generating and transporting species. To incorporate the NLO chromophore into the polymer backbone, we synthesized a NLO chromophore bearing two triflate moieties as shown in Scheme III (monomer A). The overall yield of the synthesis of monomer A was poor (<10%). After we carried out the polymerization with 2,5-bis(tributylstannyl)thiophene, a polymer (polymer III in Scheme II) was obtained in which the dominant absorption was from the nonlinear optical chromophore (Figure 1). In order to generate photocharge carriers in polymer III, it has to be illuminated at the absorbing region. However, if the NLO chromophore absorbs strongly, photochromic gratings can result. The charge carrier may come from the excitation of the NLO chromophore; the properties of the NLO chromophore will be changed. It is an undesired effect and should be avoided. Better charge generation properties are generally provided by including specific moieties to act as sensitizers. We found that the dihydropyrrolopyrroldione (DPPD) compounds are appropriate for this purpose.[18] These types of compounds have a strong absorption in the visible region, and their chemical structures are stable enough to allow us to convert them into the triflate necessary for the Stille coupling reaction. After being incorporated into the polymer chain, the compounds can form a conjugated system through the two double bonds in the DPPD system. Scheme IV shows the synthetic approach for such a monomer, monomer B.

Polymerization. The polymerization was carried out according to Scheme II, where a typical Stille catalyst system was applied. It was found in part of our other work that the reactivity of monomers with bromide or iodide was lower than the reactivity with triflate.[19] For example, the yield and the molecular weight of poly(2,5-dihexyl-1,4-phenylene-*co*-2,5-thiophene) from ditriflate are much higher than those from the corresponding diiodide. Therefore, we decided to utilize ditriflate monomers. Either Pd(PPh$_3$)$_4$ with LiCl or Pd(PPh$_3$)$_2$Cl$_2$ alone can be used as the catalyst. The reaction went on smoothly and the polymer yield was high. It is very interesting to observe that monomer B can facilitate the polymerization. It was found that polymer I, with an y/x ratio of 70/100 (see Scheme III), had a fairly high molecular weight; an intrinsic viscosity of 0.45 dL/g in NMP at 30 °C was observed. For polymers II and III, the y/x ratios are 5/95 and 0, respectively. Their molecular weights are lower than that of polymer I, and intrinsic viscosities of ca. 0.33 and 0.22 dL/g in the same condition as for polymers II and III, respectively, were obtained. Since polymers II and III are soluble in THF, GPC studies indicated that they have weight averaged molecular weights of 21 000 and 16 700 with polydispersities of 2.00 and 1.80, respectively. These results were clearly related to the electronic structures of monomer B where the existence of a DPPD ring makes this molecule electronically deficient, thus helping to activate the oxidative addition of the C–O bond of the triflate to the catalyst. Comparing our previous PR polymers with the polyurethane backbone,[10,11] these polymer exhibited much better film-forming quality. For example, a free-standing thick film (70 μm) can be easily prepared from polymer I.

Structural Characterization. Because polymer I has a much higher molecular weight, it is not soluble in chloroform-*d*, DMSO-d_6, and benzene-d_6 and only partially soluble in DMF-d_7 and chlorobenzene-d_5. However, the ^{1}H NMR spectrum in DMF-d_7 was dominated by the solvent peak and the water peak, giving little information about the structure of the polymer. The spectrum obtained from chlorobenzene-d_5 gives rise to some structural information, although the solvent peak at the aromatic region is still overwhelming. The chemical shifts due to different methyl and methylene moieties appear between 0.5 and 4.5 ppm, and the chemical shifts due to the *trans*-vinyl moiety in the nonlinear optical chromophore appear at about 6.85 and 6.95 ppm as doublets, respectively. These results indicate that the NLO chromophore was incorporated into the polymer. Polymers II and III are soluble in chloroform, and all of the features in the ^{1}H NMR spectra support the structures as proposed (see the assignments in the Experimental Section).

The FTIR spectra provide further evidence for the structures of the polymers (Figure 2). In polymers I and II, absorptions at 1662 cm^{-1} due to amide >C=O on the DPPD moieties are obvious. The intensities of this band reflect the composition of the polymers. In polymer I (with the following ratio of the DPPD/chromophore, 70/100), a very strong >C=O band can be noted; in polymer II, the >C=O band is weak. The out-of-plane deformation absorption due to the *trans*-vinyl unit on chromophore appears at 949 cm^{-1}.

(20) Teng, C. C.; Man, H. T. *Appl. Phys. Lett.* **1990**, *56*, 1734.

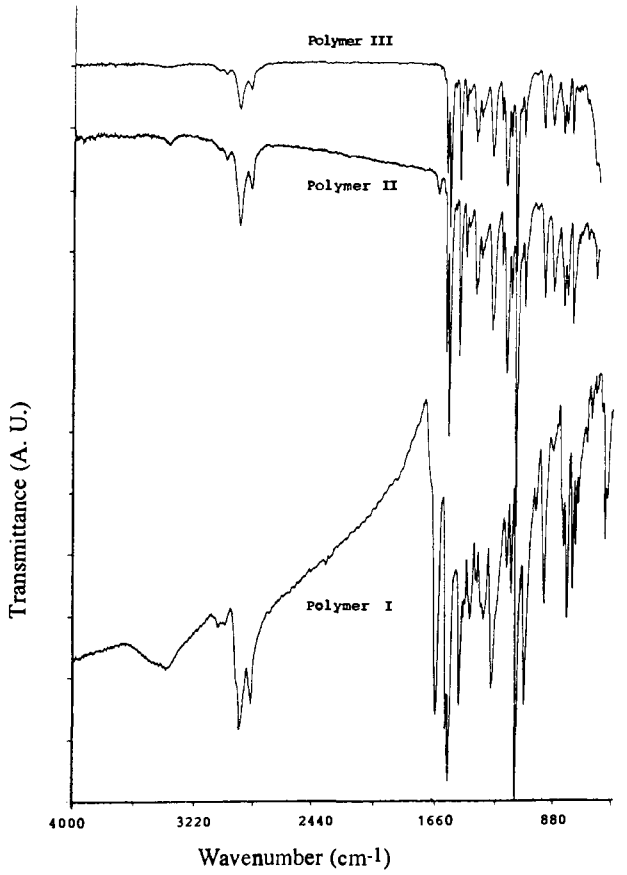

Figure 2. The FTIR spectra of polymers I–III; the spectra of polymers II and III were taken in thin films on a NaCl crystal plate and that of polymer I was taken in a KBr pellet.

Figure 1 shows the UV/vis spectra of the monomers and polymers. It can be noted that polymer III has an absorption at ca. 390 nm, mainly due to the absorption of the NLO chromophore. It is almost identical to the absorption features of monomer A, and the phenylene–thiophene backbone did not contribute much to the absorption at the near-visible region. This result is quite different from the results obtained from poly(1,4-dialkoxy-2,5-phenylene-*co*-2,5-thiophene), which shows a strong absorption at 461 nm.[15] It is caused by the increase of the twisting angle between the phenylene and the thiophenyl units. Because the phenylene ring bears such a big NLO moiety and the thiophene is a very small link unit, the steric interaction between the neighboring units, in addition to the dipole–dipole interaction, may be enough to twist the thiophene and the phenylene rings out of the planar structure, reducing the electron delocalization. Polymers I and II, however, show absorptions at 573 nm, which is dramatically shifted from the absorption of monomer B (483 nm). This is clear evidence for the incorporation of the DPPD unit into the polymers. The absorption strength is obviously correlated with the concentration of the DPPD units; the DPPD unit ratio between polymers I and II is about 75:5, which is close to the normalized absorbance ratio of polymers I and II at 573 (14:1). These results indicate that we can control the absorption strength of polymers at specific regions. This is very important for the design of photorefractive polymers. In order to demonstrate the photorefractive effect, the materials must have reasonable absorption at the wavelength of a working laser, e.g. a He–Ne laser. If the material is completely transparent, the photon cannot be absorbed, and the charge carrier cannot be excited; no PR effects can be observed. If the material has a strong absorption, the transmission of the signal will be limited. We found that polymer III has a very small absorption at the region beyond 600 nm; therefore, the grating cannot be effectivley written using a He–Ne laser. Polymer I has a strong absorption

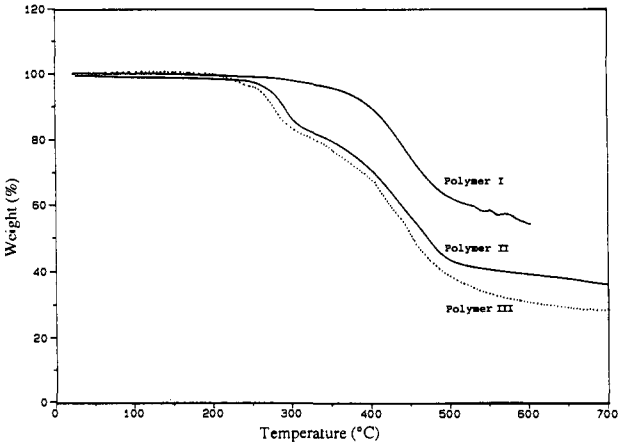

Figure 3. TGA diagrams of polymers I–III (heating rate 15 °C/min under nitrogen).

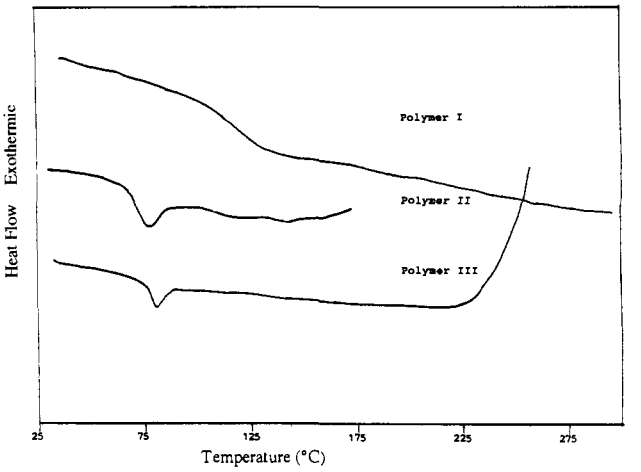

Figure 4. DSC traces of polymers I–III (heating rate 10 ° C/min under nitrogen).

at the region below 650 nm; the He–Ne laser was hardly transmitted in the thick film (90 μm). Polymer II is a more suitable material for the PR studies using a He–Ne laser to excite the material while maintaining a reasonable transmittance.

Thermal stability is a very important characterization for PR materials. TGA studies (Figure 3) showed that polymer I is the most stable polymer among the three; it started its weight loss at about 380 °C under nitrogen. For polymers I and II, two thermal weight loss processes can be noted: one at about 250 °C and the other at about 380 °C. The first one might be related to the loss of the end group because these polymers have a relatively low molecular weight. The second weight loss process might be related to the polymer backbone decomposition as for polymer I.

DSC studies revealed that polymer I exhibits a glass transition at ca 108 °C and no other thermal process was found between the temperature range of 30 and 300 °C (Figure 4). Both polymers II and III showed a sharp melting transition at about 80 °C that is clearly related to the melting of the side NLO chromophore. This transition is absent in polymer I because it has a higher density in the comonomer B and the NLO chromophore is largely isolated. For polymer II, two more transitions can be observed at ca. 105 and 143 °C. The former one is a second-order transition and coincides with the glass transition of polymer I; the latter one might be related to the backbone melting. Polarized microscopy observation showed no liquid crystal phase in any of the three polymers. These results showed that the compositions of the polymers dramatically affect the thermal properties and further affect the stability of the electrooptical effects.

Table I. Optical Properties of Polymers I–III

polymer	wt density of NLO chromophore (%)	refractive index (1064 nm)	d_{33}(1064 nm) (pm/V)	abs coeff α [λ] (cm^{-1})
I	32	1.763	54 ± 1.5	6730 [633 nm] 242 [690 nm]
II	54	1.638	89 ± 8	585 [633 nm] 201 [690 nm]
III	57	1.610	94 ± 11	120 [633 nm] 45 [690 nm]

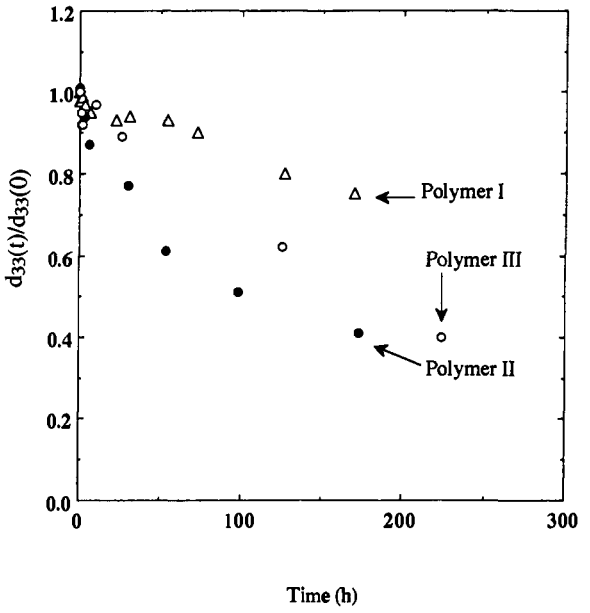

Figure 5. Temporal stabilities of second harmonic generation coefficients of polymers I–III at room temperature.

Physical Properties. To manifest the photorefractive effect, the necessary conditions are that the polymer must be photoconductive and second-order nonlinear optically active. We carried out second harmonic measurements for the electrically poled thin films of all of these polymers. Table I shows the results that indicate that these polymers have large second-order harmonic generation coefficients. Listed in the table are the weight densities of the NLO chromophore; it is clear that the $d_{33}(0)$ values are well correlated with the chromophore density. Another important characterization for second-order NLO activity is the temporal stability. Figure 5 shows the temporal stability of $d_{33}(0)/d_{33}(t)$ for these polymers, which is again well correlated to the polymer structures. Polymer I showed the highest stability among the three due to its higher glass transition temperature. Polymers II and III decayed much faster than polymer I. However, they still exhibited reasonable stability over a relatively long time, allowing photorefractive studies with no need for in situ electric poling.

To further demonstrate electrooptical (E-O) effect, the E-O coefficients were measured according to the method described in ref 20. It was found that the values of E-O coefficients have a strong dependence on the poling efficiency. For example, the thin film (ca. 0.4 μm) of polymer II showed a r_{33} value of 10 pm/V, while the thick film (3 μm) of polymer II showed a r_{33} value of only 0.4 pm/V. This is clearly caused by the inefficiency of dipole orientation in a thick film due to the limited effective electric field that can be applied.

These polymers are good insulators with very small dark-conductivity (barely detectable, instrument limit $\sim 10^{-15}$ S/cm). However, when polymers I and II were exposed to a He–Ne laser irradiation, large photocurrents were detected. The photoconductivities were found to be ca. 8×10^{-11} and 4×10^{-11} s/cm for polymers I and II, respectively. These values are comparable to those of well-known conjugated polymers, such as poly(phenylenevinylene).[21] The photocurrent was found to be field-dependent as shown in Figure 6; as the electrical field was increased, the photocurrent increased dramatically. From these results, the quantum yield of the DC photocurrent as a function of the electrical field, presented in Figure 7, can be estimated. These results can be rationalized based on Onsager's theory of germinate-pair dissociation, which will be presented elsewhere.

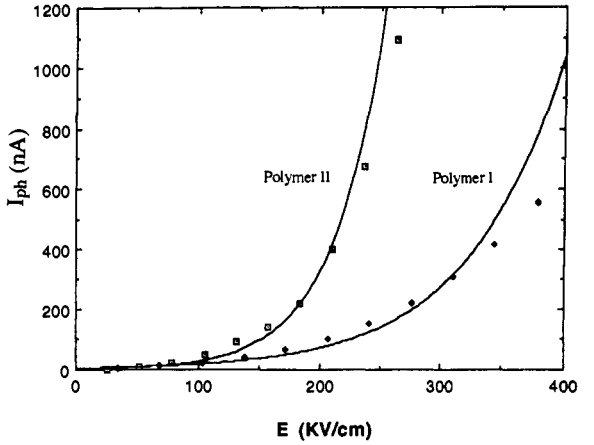

Figure 6. Photocurrents of polymers I and II as a function of external electric field strength (laser intensity, 113 mW/cm^2).

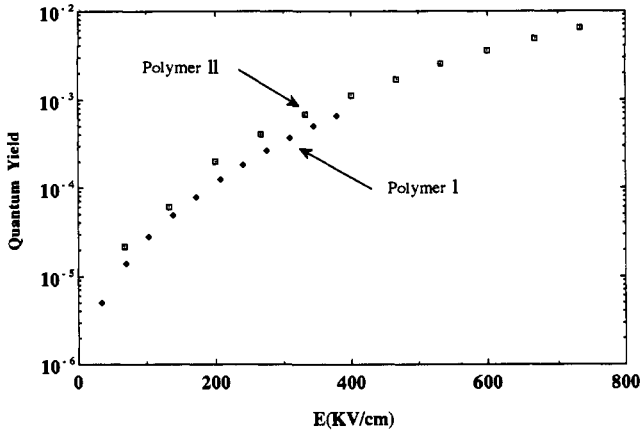

Figure 7. Quantum yields of photocharge generation of polymers I and II as a function of external electric field: (laser intensity, 113 mW/cm^2).

One important parameter for characterizing photoconductive materials is their carrier mobility. Generally, there are two methods to determine the mobility, μ, i.e. time-of-flight and xerographic discharge measurements. We applied the time-of-flight techniques to measure the carrier mobility. Figure 8 shows the typical transient photocurrent signal of the holes in both polymers I and II; the arrivals of the fastest carriers can be clearly seen. However, the initial decay and the tail of the transient signal indicated that the charge transporting was dispersive. The mobility was deduced from these experiments, which showed both temperature and field dependence (see Figures 9 and 10). It is clear from these data that the carrier mobility in polymer I is higher than that in polymer 2. As the temperature was increased, the mobility increased, indicating that it is thermally activated, with activation energies of 0.29 and 0.16 eV for polymers I and II, respectively. This activation energy difference is obviously related to the difference between the polymer compositions. However, the exact reason for this difference is not clear. The field dependence of the mobility is very interesting, as shown in Figure 10. As the external electrical field was increased, the mobility of both polymers decreased. This is in contrast with the

(21) Gailberger, M.; Bassler, M. *Phys. Rev. B* **1991**, *44*, 8643.

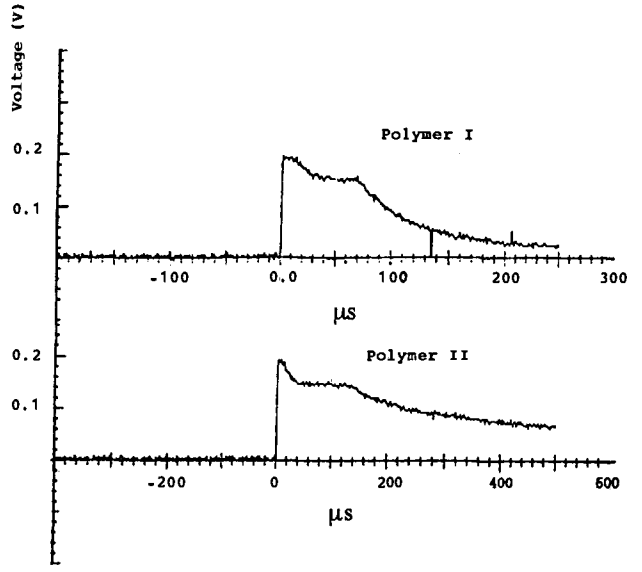

Figure 8. Transient signals of time-of-flight experiments for polymers I and II.

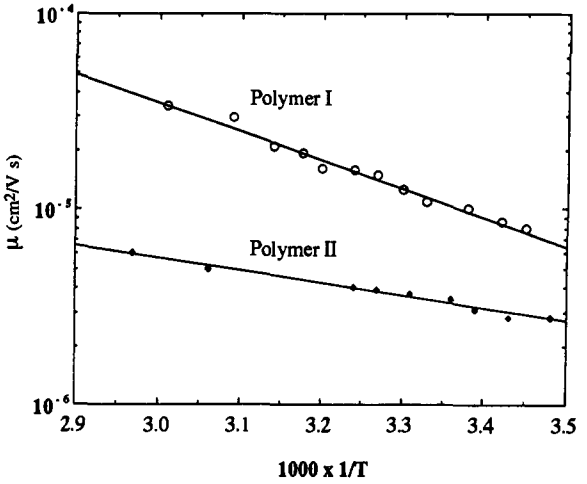

Figure 9. Charge carrier mobility as a function of temperature, (E = 552 kV/cm, laser intensity, 113 mW/cm^2).

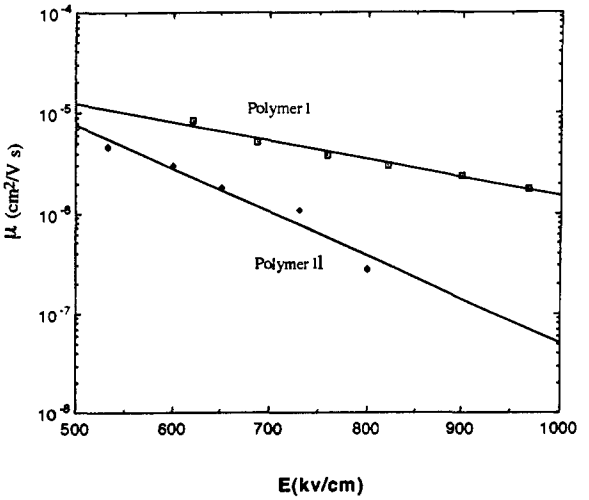

Figure 10. Charge carrier mobility as a function of external electric field (laser intensity, 113 mW/cm^2; room temperature).

results of most photoconductive composite materials, such as polyvinyl carbazole dopes with electronic donor molecules.[3] However, phenomena like this were indeed observed in a few

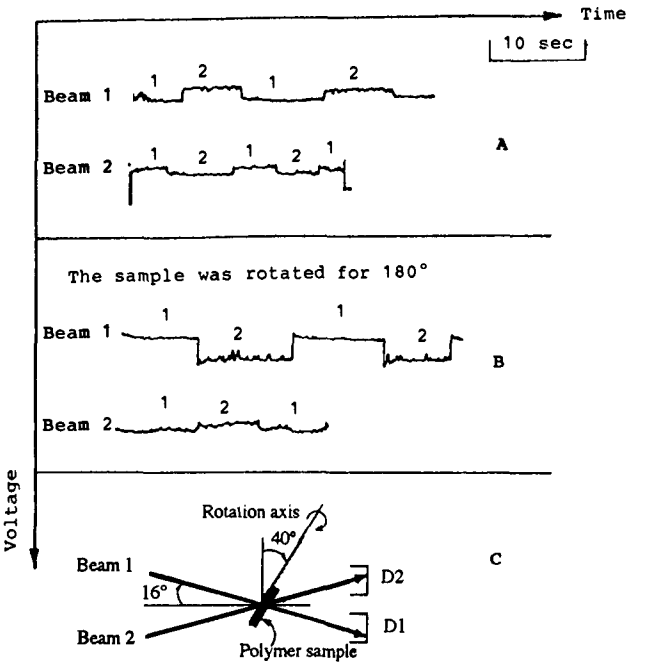

Figure 11. Two-beam coupling experimental results and setup for polymer I: (A) the polymer surface was directed to the direction of the incident beams; (B) the sample was rotated for 180 °C; (C) the two-beam coupling geometry, where D1, D2 are the diode detectors. The numbers 1 and 2 above the experimental curves indicate the number of beams intersected in the polymer samples at various stages.

composite photoconductive systems[22] and in poly(2-phenyl-1,4-phenylenevinylene) systems.[21] On the basis of the hopping model of the charge carriers, it was attributed to the random walk of the charge carrier within a random potential. The UV/vis spectra of both polymers I and II (Figure 1) showed a broad absorption region at the visible region (π–π^* transition), implying that the π-conjugated system has a wide distribution in length that caused the hole transporting state to manifest wide distributions. It is then reasonable to assume that the hole migration in polymers I and II experienced a random potential, resulting in this abnormal field dependence of the carrier mobilities.[21,22]

A very important experiment to further confirm the photorefractivity is the two-beam coupling experiment. The experimental setup is shown in Figure 11 where two incident beams, beams 1 and 2, are each diffracted by the photorefractive grafting, resulting in beam coupling. Because the polymer sample is asymmetric after electric poling, one beam should be amplified and the other attenuated if the diffraction is indeed of photorefractive nature.[23] We have performed this experiment under steady state conditions (without applying an external electric field). Figure 11 shows the preliminary experimental results where the asymmetric optical energy exchange can be clearly observed. For example, in case A, beam 1 experienced loss and beam 2 gained optical energy when the two beams were coupled. If the polymer sample was rotated for 180° around the rotation axis, the phenomenon was reversed (case B); beam 1 then had energy gain while beam 2 lost energy. Polymer film without poling showed no such effect either in two-beam or one-beam geometry on the transmitted beam intensity. This unambiguous experimental result shows that our polymers are indeed photorefractive and the photorefractive effect is very large among polymeric materials because we were able to see the asymmetric energy exchange without applying a high external electric field, an optical gain of 6 cm^{-1} was observed with intersection angle of 32°. This gain is much larger than that of our previous polymer systems.[10,11]

(22) Borsenberger, P. M.; Pautmeier; Bassler, H. *J. Phys. Chem.* **1991**, *94*, 5447.

(23) Huignard, J. P.; Marrakchi, A. *Opt. Comm.* **1981**, *38*, 249.

It can be noted that beams 1 and 2 did not increase (decrease) by the same amount. There are two reasons for this fact: a, the incident beams' intensities into the polymer film are not equal because of the unequal reflection by the tiled film; b, a in-phase absorption grating is present in addition to the 90° phase shifted index grating. Further detailed studies will be published separately.

Conclusion

In order to synthesize multifunctional polymers, especially those with oxidation and reduction sensitive moieties, the Stille coupling reaction has proven to be an effective approach. Polymers with conjugated backbones and second-order nonlinear optical chromophores have been synthesized. The expectation that these polymers will possess photorefractivity is the design idea behind the structure of the polymers. The two functionalities necessary to manifest photorefractivity, i.e. photoconductivity and electrooptical activity, have been confirmed. The primary results of a crucial experiment to confirm photorefractivity, two-beam coupling, have unambiguously demonstrated that these polymers are indeed photorefractive. The Stille reaction offers the opportunity to control, to a certain degree, the polymers physical properties, such as the charge carrier mobility, the electrooptic coefficients, the absorption windows, the quantum yield, the absorbance, etc.

Acknowledgment. This work was supported by the Air Force Office of Scientific Research (Grant No. F49620-93-1-0195) and by the National Science Foundation. Support of this work by the Arnold and Mabel Beckman Foundation through a Beckman Young Investigator Award and the Camille & Henry Dreyfus Foundation through the New Faculty Award is greatfully acknowledged. Acknowledgment is also made to the donors of the Petroleum Research Fund, administered by the American Chemical Society, for partial support of this research.